Experimental Steep, Braided Flow: Application to Flooding Risk on Fans

Dan Cazanacli[1]; Chris Paola[2]; and Gary Parker, M.ASCE[3]

Abstract: Flooding processes occurring on alluvial fans are considerably different from those occurring along single thread rivers with well defined floodplains. Active erosion, rapid sedimentation, and the uncertainty in flow path make the prediction of flood evolution and extent difficult. Based on a large scale experiment, this study investigates the long term evolution of the flow on a steep, noncohesive sediment surface resembling a complex of merged alluvial fans. The results are pertinent to the assessment of flooding hazard on alluvial fans. At any given time, the average flow occupancy was 21% of the surface. However, the flow was characterized by active channel switching and overflow processes. The percentage of the surface remaining dry was found to decay harmonically with time. A reworking time was defined as the time at which half of the surface that was initially dry remained dry, whereas the other half was inundated at least once. An empirical expression was developed in which reworking time is proportional to the average cross sectional area of flow and inversely proportional to the sediment supply.

DOI: 10.1061/(ASCE)0733-9429(2002)128:3(322)

CE Database keywords: Alluvial fans; Floods; Flood plains.

Introduction

Alluvial fans are depositional environments typically encountered at the base of a mountain front. Many, but by no means all, alluvial fans are found in semi-arid and arid regions, being prominent landscape features in the American Southwest (French 1987). Bull (1977) defines an alluvial fan as a deposit whose surface forms a segment of a cone that radiates downslope from the point where the stream leaves the sediment source area. Downstream of this point, channels are no longer incising into bedrock, and the lack of confinement creates conditions for lateral expansion of flow. Flood flows on alluvial fans vary in type including (1) essentially unchannelized sheetflows, (2) the overspilling of poorly channelized braided channels, and (3) overspill from well channelized meandering channels. In the present work, emphasis is placed on sheetfloods and overspilling braided channels, both of which are characteristic of poorly vegetated fans with little cohesive material in arid environments.

Extensive field research and reviews on alluvial fans are reported in Denny (1967), Hooke (1967), Bull (1977), Rachocki (1981), and Blair and McPherson (1994). Experimental results on alluvial fans are reported by Hooke (1967), Hooke and Rohrer (1979), Schumm et al. (1987), French (1987), and Zarn and Davies (1994). Only the last two of these studies address the issue of flood risk assessment. Flooding on alluvial fans is of increasing concern, however, as development of fans for human habitation increases.

During the spring of 1999, a stratigraphic experiment was performed in a large rectangular tank at St. Anthony Falls Laboratory, University of Minnesota. The unique feature of this experimental facility, known as the eXperimental EarthScape basin is its capacity to simulate tectonic subsidence. This is important in the context of alluvial fans because zones of subsidence tend to impound sediment, thus promoting the formation of alluvial fans. The general scope of the experiment was to simulate the stratigraphy created by fluvial deposits in a subsiding sedimentary basin. At the same time, the experiment provided an excellent opportunity to investigate the distribution of the surface flow over a steep sedimentary surface. The experiment reproduced many of the processes commonly observed in braided alluvial fans. Debris flows did not occur in the experiment discussed here.

The results from this study are pertinent to the assessment of flooding hazard on alluvial fans. Flooding processes in unconfined systems such as alluvial fans are considerably different from those occurring along single thread rivers. Frequent overflow processes and the unstable character of the channels make the prediction of flood evolution and extent difficult on alluvial fans.

The Federal Emergency Management Agency (FEMA) adopted a stochastic procedure to delineate the area of the fan that is subject to a one-percent chance of flooding (FEMA 1995). The procedure uses the total probability equation and assumes that the flow path is characterized by a "total uncertainty." The solution recommended by FEMA is based on the model developed by Dawdy (1979). Dawdy's model was critiqued by Mays and Mushtaq (1993), who characterized its assumptions as simplistic and unrealistic. The model ignores topography and does not differentiate between the active and the inactive parts of the fan. The model also assumes that channels can shift laterally at random and each point on the contour of an alluvial fan has an equal probability of being flooded. French (1992) modified this assump-

[1]Graduate Student, St. Anthony Falls Laboratory, Univ. of Minnesota, Mississippi River at 3rd Ave. SE, Minneapolis, MN 55414. E-mail: caza0002@tc.umn.edu

[2]Professor, St. Anthony Falls Laboratory, Univ. of Minnesota, Mississippi River at 3rd Ave. SE, Minneapolis, MN 55414.

[3]Professor, St. Anthony Falls Laboratory, Univ. of Minnesota, Mississippi River at 3rd Ave. SE, Minneapolis, MN 55414.

Note. Discussion open until August 1, 2002. Separate discussions must be submitted for individual papers. To extend the closing date by one month, a written request must be filed with the ASCE Managing Editor. The manuscript for this paper was submitted for review and possible publication on October 12, 2000; approved on August 14, 2001. This paper is part of the ***Journal of Hydraulic Engineering***, Vol. 128, No. 3, March 1, 2002. ©ASCE, ISSN 0733-9429/2002/3-322–330/$8.00+$.50 per page.

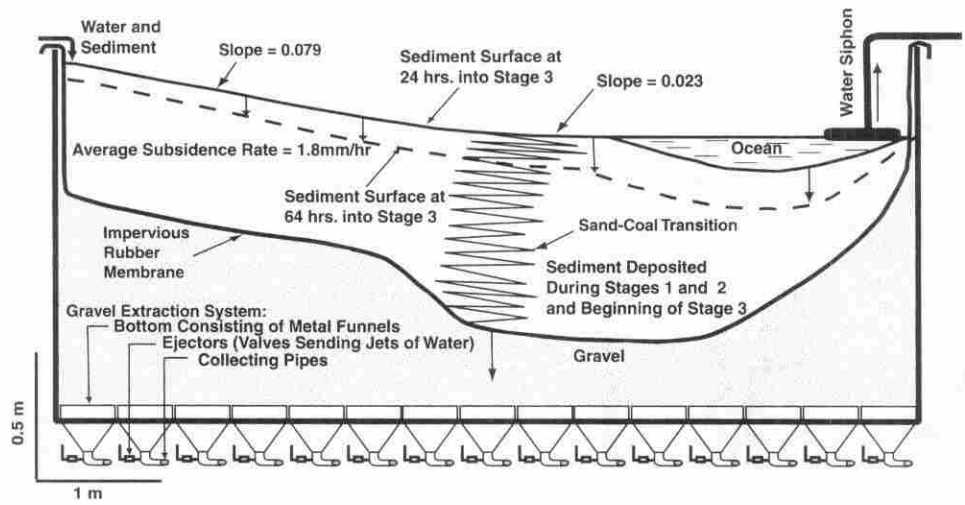

Fig. 1. Experimental tank, lateral view

tion, showing that channels have larger probability to form along the medial line of the fan than on the flanks.

In order to clarify some issues associated with alluvial fan flooding the National Research Council (NRC) established the Committee of Alluvial Fan Flooding at the request of FEMA. The committee was requested to review the definition of alluvial fan flooding and to develop criteria to determine whether an area is subject to flooding. The report issued by the committee (NRC 1997) helped distinguish alluvial fan flooding from other types of flooding that are characterized by flow path uncertainty such as deltas, pediments, and braided streams. In the case of alluvial fans, the flow path uncertainty is set by the lack of topographic confinement and by the potential for sudden deposition and erosion that may cause abrupt channel shift or overflow. In order to satisfy FEMA's objectives, the committee indicated that areas subject to alluvial fan flooding should be defined as those portions of the alluvial fans which are affected by the 100-year flood. The 100-year flood is a key concept, often used by the National Flood Insurance Program for regulation purposes. However, FEMA's objective to define the extent of the 100-year flood seems difficult to attain in the case of alluvial fan flooding. Furthermore, it appears that for at least two reasons the 100-year flood may not be an operational concept in the case of alluvial fans. First, there is no clear relationship between the magnitude of the flood and the surface that is covered by water. In the case of a stream with a well-defined floodplain, a knowledge of the discharge and the stage as well as the topography is sufficient to delineate the portion of the alluvial plain that is flooded. In the case of an unconfined river system where there is no definable floodplain, the flow path becomes highly uncertain. It is thus much more difficult to predict the surface that is affected by the 100-year flood. The extent of this surface would also depend on the partition between channel flow and sheetflow during a flood. Secondly, even if the areal extent of the 100-year flood were known, this surface would not include all portions previously affected by smaller events and therefore subject to flooding prior to 100-year flood. Conversely, since channel shift and overflow is common, smaller events could effect most of the area affected by the 100-year flood. Thus, in the case of alluvial fans, the extent of the 100-year flood is less relevant in estimating the risk associated with flooding than it is for rivers with well-defined floodplains.

The present study approaches the issue of flood risk assessment on alluvial fans from a different angle. Instead of trying to estimate the extent of one single large event (i.e., 100-year flood), the focus is shifted toward the probability that any initially dry point will be inundated in a given amount of time that can range from very short to very long intervals. In particular, the study examines the importance of lateral flow mobility in assessing the long term flood expansion on fans.

Description of Experiment

The experiment discussed here involved an area 6 m long and 3 m wide. Water and a sediment mix consisting of quartz sand and crushed coal were supplied at the upstream end of the tank. An impervious rubber membrane separated the water and sediment from the underlying infrastructure designed to reproduce tectonic effects.

The mechanics of subsidence are described in Paola (2000) and in Paola et al. (2001). The floor of the tank consists of 124 hexagonal metal funnels arranged in a honeycomb pattern. The side of each hexagon is about 0.3 m long. The lower, narrow end of each funnel is connected to a short vertical pipe (Fig. 1). Each vertical pipe is in turn connected through a right-angle elbow to a system of nearly horizontal pipes (collecting pipes). Subsidence is produced by withdrawing gravel from the vertical pipes using a short (0.1 s) pulse of water sent by a valve (ejector), which produces about 0.1 mm of subsidence (Fig. 1). The experimental deposits are produced by supplying sediment to fill the space created by extraction of the gravel.

The sediment mixture consisted of the following percentages by volume: 60% 120 μm silica (quartz), 30% 462 μ (coarse) coal, and 10% 189 μ (fine) coal. The corresponding fractions by weight are 75% silica, 19% coarse coal, and 6% fine coal. The coal has a specific gravity of 1.34, i.e., much smaller than the value of 2.65 for the sand. When submerged, the effective specific gravity of the coal was 0.34, i.e., 1/5 of that of the sand. The coal thus was a surrogate for natural fine sediments such as clay and silt, whereas the silica played the role of coarser, less mobile natural sediments such as sand and gravel.

As water and sediment were fed into the basin, a braid plain built out into standing water (Fig. 2, "ocean"). The resulting morphology is a variant of a fan delta (Nemec and Steel 1988). The base level, or water surface elevation of the body of standing water was maintained constant throughout the entire run with the

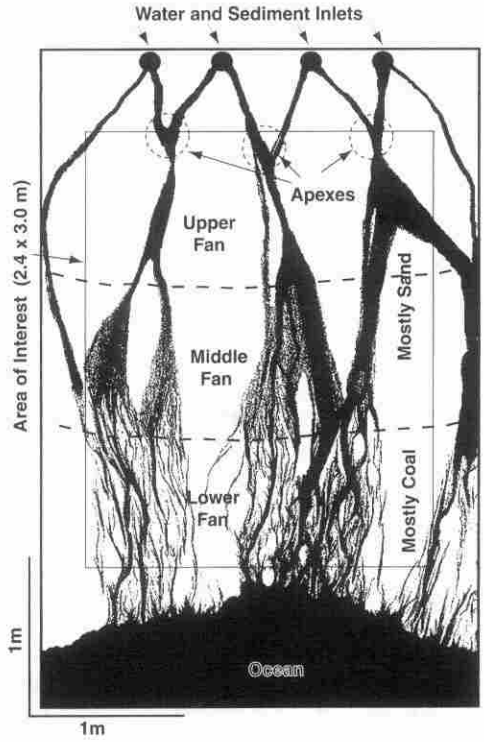

Fig. 2. Top view picture showing main flow expansion processes

aid of a siphon. The resulting shoreline equilibrated at 3.7 to 4.1 m from the upstream end of the tank (Fig. 2). The volume of sediment deposited (porosity included) was at all times kept equal to the volume of gravel extracted from below the rubber membrane as described. In other words, the rate of sediment deposition was equal to the rate of creation of accommodation space by subsidence. Under these circumstances, an equilibrium surface topography develops. It is important to note that an observer watching the flow and sediment dynamics would not realize that subsidence was taking place. The failure of the shoreline to prograde in time under conditions of constant sediment feed, however, would suggest the existence of subsidence.

The experiment consisted of four stages, each characterized by a particular mode of subsidence and by specific supply rates of sediment and water. The characteristics of each stage are summarized in Table 1. In all stages, the pattern of subsidence was extensional or hinge-like, i.e., with a subsidence rate that increased with distance from the sediment source (Allen and Allen 1990). At the onset of the experiment, the rubber membrane was slightly tilted towards the ocean (Fig. 2) at a uniform slope of approximately 0.02. After 6.5 hrs, the surface of the deposit was characterized by slope values of approximately 0.05 upstream and 0.03 downstream. In Stage 1, the subsidence also included a simulated fault located 2.2 m down the basin, as well as transverse asymmetry in the subsidence pattern. In Stages 2, 3, and 4, no fault was simulated and the subsidence was uniform in the transverse direction. In Stage 2, the rates of delivery of water and sediment were highest. In Stage 3, the water and sediment delivery rates were dropped to slightly more than one-fourth of their values of Stage 2, and the subsidence rate decreased commensurately. In Stage 4, the water discharge was doubled compared to Stage 3, but the sediment feed rate was held constant. In general, the flow consisted of overflowing braided channels or sheet flows and covered a relatively large fraction of the sediment surface.

This paper focuses mostly but not exclusively on Stage 3, during which the fraction of the surface inundated with water at any given time was about 21%, the lowest of the four stages. This fraction was low enough to be comparable to that observed on natural alluvial fan surfaces during floods. Bull (1977) indicated that large floods may at any given time cover less than 5% of the surface of large alluvial fans (>100 km^2). This fraction, however, can be 20% or larger in case of small fans (<1 km^2). During Stage 3, gravel was extracted, as explained, so that the basement was lowered at an average rate of about 1.8 mm/hr (Table 1).

Stage 3 lasted for 99 hrs, with an average thickness of accumulated sediment of 0.18 m. During the run, a downfan transition from sand to coal set up quickly and was maintained for the duration of the run. This transition was strongly reminiscent of the gravel–sand transition observed in many rivers (Sambrook-Smith and Ferguson 1995) including some on alluvial fans.

At the beginning of Stage 3, the longitudinal slope S in the upstream (proximal) sandy portion was 0.056. After about 24 hrs the surface of the sand deposit adjusted to a longitudinal slope of about 0.079 and remained essentially unchanged until the end of this stage. The downstream coal-dominated region developed an average slope of 0.023.

In addition to the data generated during Stage 3, some of the data from Stage 2 were also used to validate the scaling analysis describing the reworking of the fan surface by the flow. Stage 2 was similar to Stage 3 but the water discharge, sediment discharge, and subsidence rate values were higher by a factor of 3.7 (Table 1). The subsidence pattern during Stage 1 and the formation of incised valleys during Stage 4 effected the lateral mobility of the flow. The data from these stages were thus not used in the present study.

The surface flow was documented using a high resolution video camera and a still camera. The videotaped images provide continuous coverage and permit a good visualization of the flow kinematics. Photographs were taken every 20 min during the 99 hrs of Stage 3. In addition, a series of 98 pictures was taken at a 1-min interval starting at 34 hrs into Stage 3. A similar series of 98 pictures was also taken starting at 12 hrs into Stage 2. Since they have a much better resolution than the video images the photographs, in particular the two 98-picture series taken every minute, represent the main data base for this study.

Table 1. Experimental Conditions

Stage	Duration (hrs)	Water discharge Q_w (L/s)	Sediment discharge Q_s (g/s)	Upstream slope S	Downstream slope S	Subsidence rate σ(mm/hr)
1	40	0.40	23.82	0.050	0.029	5.3
2	30	0.51	31.43	0.060	0.017	6.7
3	99	0.14	8.40	0.079	0.023	1.8
4	48	0.28	8.40	0.063	0.029	1.8

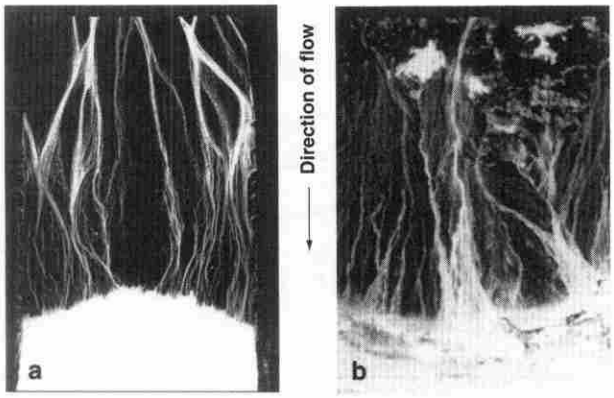

Fig. 3. Comparison between experiment: (a) and on bajada from Death Valley, Calif. (b) second image is courtesy of R. L. Hooke

Characteristics of the Surface Flow

The water and sediment were supplied through four polyvinyl chloride pipes discharging vertically into four small self-formed plunge pools (Fig. 2). The first channels initiated from the overflow from the rims of these pools. For most of the run, two or more channels emerged from each of the pools. These channels merged to form three major zones of flow confluence located between the four inlets (Fig. 2) at about 0.5 to 0.8 m from the upstream edge of the tank. At the confluence zones, the flow was relatively narrow and deep. Part of the flow from the two pools closest to either side of the tank was directed toward the sidewalls. Downstream of the three confluence zones the flow expanded, evolving into a mixture of channelized flow in braid channels and overflowing sheetflow. Each of these three confluence zones thus acted as the local apex of an alluvial fan. Although the flow expanding downstream from one apex occasionally interacted with the flow expanding from a neighboring apex within a zone 1 to 2 m downstream from the apexes, the area of investigation could be regarded as a combination of three closely spaced alluvial fans. This picture of a single fan resulting from the merging of smaller fans originating from point sources [Fig. 3(a)] could, for field cases, be analogous to a bajada. A bajada consisting of merging fans from Death Valley, Calif. is shown in Fig. 3(b).

To facilitate further discussion, the surface of the deposit is somewhat arbitrarily divided into three regions: upper (proximal) fan, middle (medial) fan, and lower (distal) fan (Fig. 2). The flow constantly reworked the surface of the fan. The reworking was accomplished by overflow as well as several channel shifting mechanisms. Three such modes were prominent: a single channel making a sudden jump, or avulsion to a new position; a channel bifurcation; and a channel migrating gradually, through bank erosion, into a new position. Most of the avulsions and bifurcations occurred in the upper fan area. To a large extent, these rapid flow switching mechanisms determined the flow pathways farther downstream.

Avulsions are common in distributary environments such as river deltas or alluvial fans (Bull 1977; Schumm et al. 1987; Bryant et al. 1994). In the experiment reported here, a common mode of avulsion was associated with the migration of channel bends. This migration often increased channel curvature locally. The flow then breached through the outer bank and suddenly shifted (Fig. 2). A similar mechanism was observed by Zarn and Davies (1994) in their laboratory experiment.

Bifurcations occurred as the water overtopped the channel banks and expanded laterally. The triangular-shaped sheet flow resulting from expansion in the upper fan evolved into two distinct channels in the middle fan. These channels developed on each side of the previously existing channel. In most cases, the antecedent channel filled up with sediment and was abandoned. However, cases where two or even three channels coexisted were also common. The flow expansion was associated with the formation of erosional scour holes. A hydraulic jump developed at the scour hole indicating supercritical flow conditions. These scour holes typically migrated upstream at rates of about 5 to 10 mm/s. This pattern of upstream-migrating scour holes appears to be a two-dimensional analog of the one-dimensional transportational cyclic steps [discussed in Taki and Parker (unpublished 2000) and Sun and Parker (unpublished 2000)].

Lateral channel migration through bank erosion was the most common mechanism for channel shifting in the middle fan area. The channels shifted laterally through bank erosion at rates varying from millimeters to centimeters per second. Many of the more rapid channel migrations consisted of a combination of bank erosion and overflow. As the channel eroded into one of its banks, overbank flow took place simultaneously. The relatively wide, shallow sheetflow generated in this way moved laterally. The flow often eventually regrouped into a new channel (Fig. 2).

Most of the silica sand sediment, which represented 60% of the total sediment input at the upstream end, deposited in the upper and middle fan areas. While these areas had an average slope of about 0.079, the lower fan area had an average slope of only 0.023 (Fig. 1). The changes in flow distribution in the lower fan region were dictated almost entirely by changes occurring upstream. As the wider channels formed in the upper and middle areas of the fan entered the lower fan area, the combination of higher bed roughness and lower sediment concentration forced the flow to organize into more numerous but narrower channels. The channels in the lower fan area repeatedly divided and rejoined forming a classical braided stream pattern (Fig. 2).

Representative images of the flow distribution and examples of the processes mentioned above can be seen in a video clip available at the web site http://www.umn.edu/safl/research/JT_flow.html.

Data From Still Pictures

In order to obtain a good color contrast between the flowing water and the sediment surface, an opaque blue dye was added to the water at a concentration of 0.05% (by volume). All pictures were digitized at the maximum resolution (2048×3072 pixels). Corrections were applied for radial distortion and perspective view. The pixel size was about 1.5 mm. The area captured by the photocamera covered the entire width of the basin and 75% of the length, i.e., leaving out 0.5 m at the upstream end and 1 m at the downstream end.

Since it was not practical to analyze the data using full resolution photos, the information was processed and stored in a more compact form. The area of interest was defined for the purposes of this study to be the rectangular area approximately 2.4 m×3 m starting 0.6 m downstream of the water-sediment feeding points at the upstream margin of the tank, and 0.3 m from each lateral margin (Fig. 2). The flow along the side walls, the zone upstream from the self-formed apexes discussed previously, and the downstream part of the tank containing standing water were not included in the analysis. The area of interest was divided into a grid

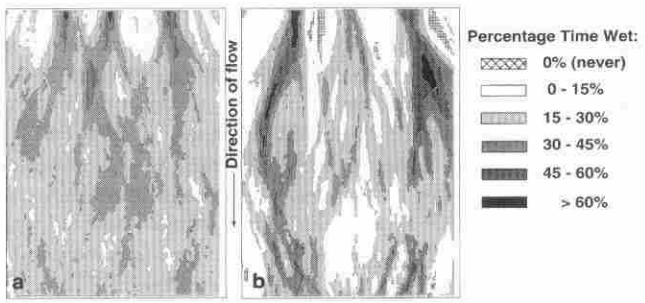

Fig. 4. Percentage time wet computed for 16 hrs (a) and 98 min (b) of run during stage 3

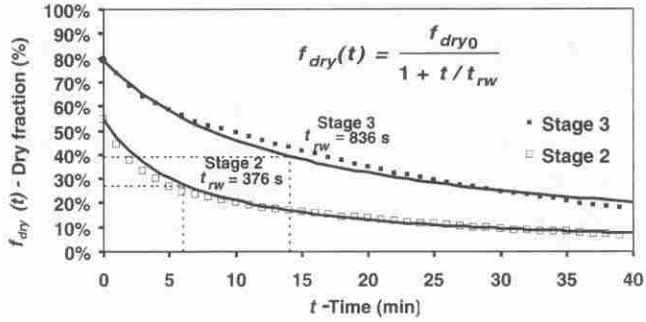

Fig. 5. Reduction of dry fraction of surface with time

of 80×100 squares with sides approximately 3 cm long. The color information within each of these squares in each image was analyzed. If the majority of the pixels within the square were blue the square was assigned the value 1, i.e., "wet". Conversely, if the majority of pixels within the square were black and/or white, the square was assigned the value 0, i.e., "dry". Using a large number of consecutive images, an average value was calculated for each square. These averaged values approximate the fraction of time each square was wet. Figs. 4(a and b) indicate the percentage of time for which each of the squares was wet for time intervals of 16 hrs and 98 min (approximately 1.6 hrs), respectively. Fig. 4(a) indicates that, apart from the upper fan region, the flow distribution averaged over 16 hrs was relatively uniform in the transverse direction, indicating that the channels shifted laterally numerous times. This is likely the case in field fans over sufficiently long time scales, since the channels must eventually carry and deposit sediment over the entire surface of the fan. Fig. 4(b), however, shows that over the shorter period of time the flow tended to concentrate in certain areas. For the majority of time the flow was concentrated in triangular areas with acute angles of 25°–30° and vertex located at the apex of the fan. Note that almost the entire surface was flooded at least once within 98 min.

Flow Distribution Statistics

At any given instant, only a fraction of the surface of the fan was inundated with water flowing in channels or as sheet overflow. Over time, however, every point on the fan was repeatedly inundated and received deposited sediment. As subsidence created accommodation space for sediment deposition, that space was occupied so rapidly that no visible depressions ever appeared on the surface. Evidently, then, the time scale of the process of fan surface reworking was in some sense rapid compared to the time scale of subsidence.

The data obtained from the photos can be used for flood risk assessment on alluvial fans. The statistical analysis of the flow distribution on the fan surface was done using the photos taken every minute starting at 34 hrs into Stage 3 and at 12 hrs into Stage 2. Both series consist of 98 photos. As the scaling analysis presented later will indicate, 98 min of experiment time corresponds to a real time interval in the order of hundreds of years or more. Longer time intervals are indeed beyond any practical concern in a risk assessment, in that Fig. 4(b) shows that most of the surface was flooded at least once during the 98 min interval.

Consider a field hydrologic and geomorphic investigation carried out on a particular alluvial fan that has designated all areas affected by recent floods as wet and the remaining area as "non-flooded" or "dry." Two main questions can be addressed: (1) How much of the area perceived as dry would be affected by the subsequent floods?, and (2) Which dry zones would be affected first? The former question is essentially quantitative, whereas the latter is qualitative. These issues were addressed using the 1-min interval photographs from Stage 3 of the experiment. Additional information was obtained using the corresponding set of 1-min photographs from Stage 2.

At the beginning of any time interval, time t was set equal to zero and the fractions of fan area that were wet and dry were recorded. The initial fraction of fan area that is dry is here denoted as f_{dry0}. At starting time, $t=0$ during Stage 3, the average fraction of fan that was dry was about 79%; thus, at any given instant, about 21% of the fan surface was inundated by either channelized flow or sheet overflow. For Stage 2, the parameter f_{dry0} was found to be equal to 0.55. The fraction of fan area $f_{dry}(t)$ that remained dry (i.e., was not inundated) since $t=0$ was recorded as a function of t (Fig. 5). Note that the dry fraction continuously decreased with time as the flow expanded into regions not flooded since $t=0$. During Stage 3, after 40 min, only 17% of the fan surface had not been wet at least once since $t=0$.

The data thus indicate that given enough time, the entire fan surface was eventually flooded at least once. The reduction of dry fraction with time was not linear, instead decaying in a crudely exponential fashion. However, the data could be better fitted to a relation of harmonic form, i.e.,

$$f_{dry}(t) = \frac{f_{dry0}}{1+mt} \tag{1}$$

Relation (1) can be rewritten in a useful way. Let t_{rw} (reworking time)=the average time required for the fraction f_{dry} to decline from f_{dry0} to $f_{dry0}/2$. It is immediately seen from Eq. (1) that t_{rw} must be equal to the inverse of m, so that the equation can be rewritten as

$$f_{dry}(t) = \frac{f_{dry0}}{1+\dfrac{t}{t_{rw}}} \tag{2}$$

The parameter t_{rw} can thus be regarded as a characteristic decay time for the fraction that is dry. That is, after a period of time equal to t_{rw} the original dry fraction was reduced to half. After one more t_{rw} period, the dry fraction was reduced to one third, and so on.

For Stage 3, the average value of t_{rw} is 836 s, whereas for Stage 2 the average value of t_{rw} is 376 s (Fig. 5). This value is determined by the specific conditions of the experiment.

To apply these results to the field, it is important to correctly identify the parameters that determine the value of t_{rw}. This value is a measure of the rate at which the flow shifts from one location to another across the fan, i.e., the rate at which the fan surface is reworked. We approach this issue with the aid of a simple dimensional scaling. Consider a transverse transect across the fan. Let B_t denote the total width of the fan across the transect and B_a denote the average width across the transect that is actively inundated with water from either a channel or a sheet overflow at any given time. The ratio between these two parameters can be approximated as

$$\frac{B_a}{B_t} = 1 - f_{\text{dry0}} \tag{3}$$

The time t_{rw} required to reduce the initially dry area by half thus can be estimated as

$$t_{rw} = \frac{1}{2}\frac{B_t - B_a}{v_s} \tag{4}$$

where v_s=an appropriately defined velocity of transverse shift of flow that drives reworking.

We estimate the parameter v_s as follows. Let H=the average flow depth in the inundated area. Based on the observations presented in the previous section, the rate at which the active flow migrates laterally appears to be controlled by flow expansion processes in the upper fan region. To a large extent it is sediment deposition in the upper fan region that forces the flow to move laterally and invade new areas. The rate of lateral migration of the flow can thus be considered to be proportional to the rate of channel infilling. The rate of channel infilling in turn scales with the volume sediment transport rate Q_s divided by the cross sectional area B_aH of the zone that must be filled in order to drive channel shift. Thus

$$v_s \propto \frac{Q_s}{B_a H} \tag{5}$$

and finally

$$t_{rw} = \beta \frac{B_a H (B_t - B_a)}{Q_s} \tag{6}$$

where β=a dimensionless coefficient of proportionality.

In principle, the coefficient β could in turn depend upon other dimensionless parameters, e.g., the slope S and the Froude number of the flow **F**. If the form of Eq. (6), however, parameterizes the dominant processes driving channel shift, it might be expected that β could be approximated by a relatively constant value that is of the order of unity. This value might then be presumed to be valid for unvegetated fans constructed from noncohesive material at any size scale.

While the experiment does not allow for the testing of Eq. (6) over a broad range of flow conditions, the measured values of t_{rw} and other parameters of Stage 2 and Stage 3 do allow for a first evaluation of β. The value of B_t was taken to be 2.4 m, or the width of the interest as previously defined (Fig. 2) in both cases. The values of B_a were computed using Eq. (3) from the measured values of f_{dry0} of 0.79 (Stage 3) and 0.55 (Stage 2).

The average flow depth, H, was indirectly determined using the assumption that the flow was slightly supercritical. Grant (1997) showed that unconfined flow over a steep noncohesive surface tends to be just slightly supercritical. Choosing a value of 1.05 for the Froude number, the value of the average depth of flow, H, was calculated from:

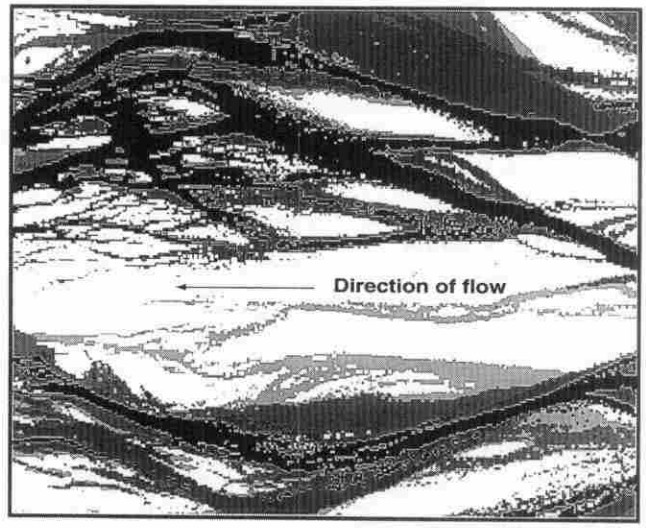

Fig. 6. Flood expansion in time: black—areas flooded at time $t=0$; gray—areas inundated within following 5 min (dark gray), 10 min (medium gray), and 15 min (light gray); white—areas still dry after 15 min

$$\mathbf{F} = \frac{U}{\sqrt{gH}} \tag{7}$$

where g=the acceleration of gravity, and the continuity equation:

$$Q_w = B_a H U \tag{8}$$

where Q_w=the water discharge.

H was found to be 1.7 mm for Stage 3 and 2.5 mm for Stage 2. The values of Q_s were 3.9 cm^3/s (Stage 3) and 14.8 cm^3/s (Stage 2). The values of β back calculated from Eq. (6) using these numbers are 2.01 (Stage 3) and 1.56 (Stage 2). The fact that these values are not only fairly close to each other, but also are of order one lends some credence to the generality of the form (6).

In order to estimate which of the zones perceived as dry at a given moment would be first effected by subsequent floods, the average waiting time for any dry point on the fan to be inundated was determined. Fig. 6 shows a typical example of how the fan area is progressively flooded. At any given moment in Stage 3, about 21% of the surface was covered by water whereas the remaining 79% of the surface was dry, i.e., not inundated at the time. About 15 min later, only half of this portion (i.e., 39.5% of the surface) was still dry, i.e., never inundated during the previous 15 min. Fig. 6 suggests that given a certain area that was "recently flooded," i.e., inundated at time $t=0$ (black areas), the subsequent floods are likely to expand in the immediately adjacent zones (dark gray areas), and then move progressively into more distant areas (medium and light gray areas). As appears from Fig. 4(b) over a significant period of time, most of the flow is contained within a triangular domain with an acute angle of about 25°–30° and the vertex at the apex of the fans. Thus, the spatial distribution of the subsequent floods is very loosely predictable. There are less frequent events in which a sudden change in channel direction, e.g., an avulsion, effects areas that are more distant relative to the initial inundated zone. Observation of the patterns of shifting during the experiment suggests that channels which attain a high curvature are more likely to avulse. These qualitative observations, when combined with a detailed look at the topography and the use of more advanced flow analysis programs (O'Brien 1993; May and Mushtaq 1993) may be of some

use in estimating where inundation might next occur in the field. The evidence presented thus suggests that while being far from predictable in a deterministic sense, the problem of risk of flooding on alluvial fans is amenable to statistical characterization. In addition, the zones most likely to be inundated by the next flood can be at least qualitatively inferred.

Scaling Up Results

The results of the previous section may be used to make estimates of the long-term impact of major flood events in natural alluvial systems. Here, the results of the present experiment are scaled up to field scale using the principles of distorted Froude modeling (e.g., Graf 1971). The field-scale river system is assumed to have the same configuration as the experiment. In addition, it is assumed to be either unvegetated or so sparsely vegetated that vegetation does not restrict channel mobility during floods. Finally, it is assumed that the sediment on the fan has no cohesion.

With this in mind, let $1:\lambda_v$ represent the vertical scale ratio and $1:\lambda_h$ represent the horizontal scale ratio. According to distorted geometric modeling, the following relationships apply between field prototype values (P) and laboratory (M) values.

$$\text{Fan length } L \quad L_P=\lambda_h L_M \tag{9}$$

$$\text{Average fan width } B_t \quad B_{tP}=\lambda_h B_{tM} \tag{10}$$

$$\text{Area of the fan } A \quad A_P=\lambda_h^2 A_M \tag{11}$$

$$\text{Downstream bed slope } S \quad S_P=\frac{\lambda_v}{\lambda_h} S_M \tag{12}$$

$$\text{Average depth of inundation } H \quad H_P=\lambda_v H_M \tag{13}$$

$$\text{Aggregate width of the active channels } B_a \quad B_{aP}=\lambda_h B_{aM} \tag{14}$$

Relation (14) implies that the ratio B_a/B_t, which is a close approximation of the fraction of surface that is flooded at any given time, is the same in the prototype as in model. Using Stage 3 as a basis for inference, it is not uncommon that 20% or more of the surface of small alluvial fans is covered by water during major flood events (Bull 1977).

Froude similarity is realized when the Froude number (7) is the same in the prototype as it is in the model

$$\frac{U_P}{\sqrt{gH_P}}=\frac{U_M}{\sqrt{gH_M}} \tag{15}$$

Combining Eq. (15) with Eq. (13), the average flow velocity scales as

$$U_P=\lambda_v^{1/2} U_M \tag{16}$$

Water discharge satisfies the equation of continuity, so that

$$Q_w=UB_aH \tag{17}$$

Combining Eqs. (13), (14), (16), and (17), then,

$$Q_{wP}=\lambda_h\lambda_v^{3/2} Q_{wM} \tag{18}$$

Combining Eqs. (6), (10), (13), and (14), the time for reworking t_{rw} scales as

$$t_{rwP}=\beta\frac{\lambda_h B_{aM}\lambda_v H_M \lambda_h (B_{tM}-B_{aM})}{Q_{sP}}=\lambda_h^2\lambda_v\frac{Q_{sM}}{Q_{sP}} t_{rwM} \tag{19}$$

These results apply to a system that is continuously in flood. While this was the case in the model experiment, it is not the case in the field, for which morphologically significant flooding is a rather rare event. In order to extrapolate the results of the experiment to field scale, it is important to accurately estimate the fraction of time a fluvial system is subject to a morphologically significant flood event. While floods in the field vary in intensity and duration, here it is useful to simplify the description to a single "effective" flood event with a specified flow and sediment discharge, duration, and recurrence frequency. Here, the recurrence frequency is quantified in terms of an intermittency I denoting the fraction of time that the fan is morphologically active (Paola 1990).

Relation 19 must then be modified to incorporate the intermittency

$$t_{rwP}I=\lambda_h^2\lambda_v\frac{Q_{sM}}{Q_{sP}} t_{rwM} \tag{20}$$

According to this relation, t_{rwP}=the actual average time of reworking in the prototype, including the "down" time when the fan is either completely dry or morphologically inactive (e.g., under low flow conditions).

One way to estimate the value of I is from flood records. However, because on many alluvial fans floods are episodic events occurring in rather remote areas, they are poorly documented. Alternatively, assuming that the fluvial system has achieved an approximate steady state at which the shape of the longitudinal profile remains unchanged (Hooke and Dorn 1992), the intermittency can be estimated from the following mass balance equation

$$Q_{sP}I=(1-n_P)a_P A_P \tag{21}$$

where a_P represents the average sediment accumulation rate and n represents the porosity.

In the experiment, the streams were always in flood, so that $I=1$ and Eq. (21) takes the form

$$Q_{sM}=(1-n_M)a_M A_M \tag{22}$$

Combining Eqs. (11), (21), and (22), and assuming $n_P=n_M$, the prototype intermittency can be computed as

$$I=\lambda_h^2\frac{Q_{sM}}{Q_{sP}}\frac{a_P}{a_M} \tag{23}$$

Combining Eqs. (20) and (23), the prototype value for t_{rw} becomes:

$$t_{rwP}=\lambda_v\frac{a_M}{a_P} t_{rwM} \tag{24}$$

Sediment grain size can be also scaled by setting dimensionless Shields shear stress at flood flow in the prototype equal to the corresponding value in the model

$$\tau_P^*=\tau_M^* \tag{25}$$

Here, the Shields stress is estimating using the normal flow approximation for boundary shear stress

$$\tau^*=\frac{HS}{D(\rho_s-\rho)/\rho} \tag{26}$$

in which D=the median grain size and ρ_s and ρ=the densities of sediment and water, respectively. Combining Eqs. (25) and (26) with Eqs. (12) and (13), we obtain

$$D_P=\frac{\lambda_v^2(\rho_{sM}-\rho)/\rho}{\lambda_h(\rho_{sP}-\rho)/\rho} D_M \tag{27}$$

Table 2. Scaling Model: Numerical Results

Parameter	Units	Model (M)	Prototype (P)	Equation
Horizontal scale—λ_h	—	1:1000		assumed
Vertical scale—λ_v	—	1:400		assumed
Fan length—L	m	3	3000	9
Fan width—B_T	m	2.4	2400	10
Slope—S	—	0.079	0.032	12
Fraction dry—f_{dry0}	—	0.79	0.79	assumed
Aggregate flow width—B_A	m	0.504	504	6
Froude number—**F**	—	1.05	1.05	assumed
Average flow depth—H	m	1.7×10^{-3}	0.68	13
Water discharge—Q_w	m^3/s	109.0×10^{-6}	872	18
Average flow velocity—U	m/s	0.13	2.54	16
Sediment density—ρ_s	kg/m^3	2650	2650	assumed
Median grain size—D	m	0.1×10^{-3}	17.6×10^{-3}	27
Sediment porosity—n	—	0.35	0.35	assumed
Average aggradation rate—a	m/s	0.5×10^{-6}	31.7×10^{-12}	assumed
	mm/year	15.8×10^{3}	1	
Reworking time—t_{rw}	s	836	5.3×10^{9}	24
	years	26.5×10^{-6}	167	

Numerical Exercise

Consider a hypothetical field alluvial fan with scaling factors λ_h and λ_v of 1:1000 and 1:400. According to Eqs. (9)–(12), the geometry of this hypothetical prototype fan is defined by a length of 3 km, a width of 2.4 km, and a slope of 0.032 (1.8°) in the upper portion and 0.009 (0.5°) in the lower portion. Scaling analysis numerical results are summarized in Table 2.

All values for the model (Table 2) were either imposed or measured directly from the experiment, except for the average depth of inundation, H_M which was indirectly determined as explained. All values for the prototype were either assumed or calculated using the aforementioned equations. The following assumptions were made: The fraction of surface that was dry at any given moment during the flood was the same in prototype as in the model ($f_{dry0}=0.79$). The porosity values were also considered to be the same ($n=0.35$, as measured in the experiment). The flow in the prototype was considered to be slightly supercritical (**F**=1.05). Finally, the choice for the aggradation rate for the prototype is based on work done by Hooke (1972), who estimated average sedimentation rates for several alluvial fans in Death Valley at about 1 mm/year.

Using the experimental value of t_{rwM} reported in Table 2, it is found from Eq. (25) that the resulting value for t_{rwP} based on scaling analysis is 167 years. This value seems rather large. However, many alluvial fans are found in arid and semi-arid regions where intense precipitation events are rare, resulting in a small intermittency. In addition, in this numerical exercise, the entire area of the prototype fans is considered to be active. In reality, large portions of natural alluvial fans could be inactive for thousands of years. French and Fuller (1993) defined criteria to distinguish the active portions from the inactive ones. If only a fraction of the fan area is active, the flow would be restricted to this portion only and the resulting value of t_{rwP} would be smaller.

Conclusions

The experiment provides a basis for characterizing the processes by which a sediment-laden flow reworks the sediment surface. The experimental results are used to describe the processes of avulsion, bifurcation, and channel migration that drive reworking. They are also used to obtain estimates of (1) the fraction of the surface that is inundated at any given time and (2) the decrease in time of the fraction of sediment area that has never been inundated since some specific starting time. These results in turn allow the determination of functional forms that characterize the risk of inundation.

The results are applied to field-scale fluvial fans using the principles of distorted Froude modeling and the relation (6) characterizing the average time of reworking. The application of Eq. (6) to field scale is reasonable but unverified, and is thus the most tentative part of the analysis. This notwithstanding, the model appears adequate to describe the dynamics of reworking and the risk of flooding on a range of small unvegetated or sparsely vegetated field-scale fans built from noncohesive sediment in an arid environment, and subject to infrequent but extreme floods. In particular, analysis of the results of the experiment suggests the following:

1. Channel shift processes such as avulsions and channel bifurcation occur primarily in the upper fan region. Changes in flow path in this region have a major impact on the flow distribution downstream;
2. When averaged over long periods of time (e.g., thousands of years or more at prototype scale), distribution of the flow and sediment deposition across the surface is relatively uniform. However, over shorter periods of time, the flow tends to concentrate in specific areas, whereas other areas are only sporadically flooded;
3. Estimating the reduction of the dry fraction (i.e., percentage surface not affected by flooding since some arbitrary time $t=0$) with time may provide an improved approach to the evaluation of the risk associated with alluvial fan flooding. The reduction of the dry fraction is not linear with time, but rather can be approximated by a harmonic law (Fig. 5). The characteristic time for the reduction of the dry fraction is proportional to the average cross sectional area of the flow and inversely proportional to the sediment supply; and
4. At any given moment, the areas where the flow is most

likely to expand during the next major flood events are those areas affected by recent floods and their immediate vicinity. (Fig. 6).

The results of this study indicate that lateral mobility could be at least as important as flood extent in determining what areas of a fan are at risk from flooding. We certainly do not claim that we have devised a complete new approach to the evaluation of the risk of flooding on alluvial fans. Rather, we hope that the line of thinking outlined here can in future years be extended so that it does become both truly predictive, as well as sufficiently accurate for application in the field.

Acknowledgments

This study would not have been possible without a team effort that included many colleagues at St. Anthony Falls Laboratory. The writers are particularly indebted to Jim Mullin and Chris Ellis who built the experimental facility and made sure that all its technical components were working properly. The writers would like to thank Ben Sheets, John Swenson, and Jeff Marr for their valuable help during the experiment. Special thanks are due to Tom Hickson and Ben Erickson for their helpful input with image processing. This study is based in part on the Master of Science thesis of the first writer. It was supported by National Science Foundation Grant No. EAR 9725989.

Notation

The following symbols are used in this paper:

A = fan area;
a = sediment aggradation rate;
B_a = aggregate width of active channels and sheetflow;
B_t = total width of fan;
D = median grain size;
$f_{\mathrm{dry}}(t)$ = fraction of fan surface that remains dry as function of time;
f_{dry0} = average fraction of fan surface that is dry at arbitrary time;
$\mathbf{F}$ = Froude number;
g = gravitational acceleration;
H = average inundation depth;
I = intermittency;
L = length of fan;
M = subscript denoting model (experiment) value; and
m = fitting parameter;
n = sediment porosity;
P = subscript denoting prototype (field) value.
Q_s = sediment discharge;
Q_w = water discharge;
S = slope;
t = time;
t_{rw} = reworking time;
U = average flow velocity;
v = velocity of transverse shift of flow;
β = dimensionless scaling parameter;
λ_h = horizontal scale factor;
λ_v = vertical scale factor;
ρ = water density;
ρ_s = sediment density;
σ = subsidence rate; and
τ^* = dimensionless Shields stress.

References

Allen, P. A., and Allen, J. R. (1990). *Basin analysis, principles and applications*, Blackwell Scientific, Oxford, U.K.

Blair, T. C., and McPherson, J. G. (1994). "Alluvial fan processes and forms." *Geomorphology of desert environments*, A. D. Amrahams and A. J. Parsons, eds., Chapman and Hall, London, 354–402.

Bryant, M., Falk, P., and Paola, C. (1995). "Experimental study of avulsion frequency and rate of deposition." *Geology*, 23(4), 365–368.

Bull, W. B. (1977). "The alluvial fan-environment." *Progress in Physical Geography*, 1, 222–270.

Dawdy, D. R. (1979). "Flood frequency estimates on alluvial fans." *J. Hydrologic Eng.*, 105(HY11), 1407–1413.

Denny, C. S. (1967). "Fans and pediments." *Am. J. Sci.*, 265, 81–105.

Federal Emergency Management Agency (FEMA) (1995). "Appendix 5: Studies of alluvial fan flooding. Guidelines and specifications for study contractors." *Doc. No. 37*. Washington, D.C.

French, R. H. (1987). *Hydraulics processes on alluvial fans*, Elsevier, Amsterdam, The Netherlands.

French, R. H. (1992). "Preferred directions of flow on alluvial fans." *J. Hydrologic Eng.*, 118(7), 1002–1013.

French, R. H., Fuller, J. E., and Waters, S. (1993). "Alluvial Fan: Subset definitions." *Engineering Hydrology: ASCE Hydraulics Div., Proc., Symposium*, Y. K. Chin, ed., 276–281.

Graf, W. H. (1971). *Hydraulics of sediment transport*, McGraw-Hill, New York, N.Y.

Grant, G. E. (1997). "Critical flow constrains flow hydraulics in mobile-bed streams; a new hypothesis." *Water Resour. Res.*, 33, 349–358.

Hooke, R. L. (1967). "Processes on arid-region alluvial fans." *J. Geol.*, 75, 438–460.

Hooke, R. L. (1972). "Geomorphic evidence for Late-Wisconsin and Holocene tectonic deformation, Death Valley, Calif." *Geol. Soc. Am. Bull.*, 83, 2073–2098.

Hooke, R. L., and Dorn, R. I. (1992). "Segmentation of alluvial fans in Death Valley, California: New insights from surface exposure dating and laboratory modelling." *Earth Surf. Processes Landforms*, 17, 557–574.

Hooke, R. L., and Rohrer, W. L. (1979). "Geometry of alluvial fans: effect on discharge and sediment size." *Earth Surf. Processes Landforms*, 4, 147–166.

Mays, L. W., and Mushtaq, H. (1993). "Hydraulic modeling of alluvial plains (slopes) and alluvial fans using DAMBRK." *Engineering Hydrology: ASCE Hydraulics Div., Proc., Symposium*, Y. K. Chin, ed., 270–275.

National Research Council (NRC). (1997). "Alluvial fan flooding." *Water Science and Technology Board*, National Academy, Washington D.C.

Nemec, W., and Steel, R. J. (1988). "What is a fan-delta and how we recognize it?" *Fan Deltas: Sedimentology and Tectonic Settings*, W. Nemec and R. J. Steel., eds., Blakie, London, 11–17.

O'Brien, J. S. (1993). "Two-dimensional flood hazard simulation on alluvial fans." *Engineering Hydrology: ASCE Hydraulics Div., Proc., Symposium*, Y. K. Chin, ed., 264–269.

Paola, C. (1990). "A simple basin-filling model for coarse-grained alluvial systems." *Quantitative Dynamic Stratigraphy*, T. A. Cross, ed., Prentice-Hall, Englewood Cliffs, N.J., 363–374.

Paola, C. (2000). "Quantitative models of sedimentary basin filling." *Sedimentology*, 47, Suppl. 1, 121–178.

Paola, C., Mullin, J., Ellis, C., Mohrig, D. C., Swenson, J. B., Parker, G., Hickson, T., Heller, P. L., Pratson, L., Syvitski, J., Sheets, B., and Strong, N. (2001). "Experimental stratigraphy." *GSA Today*, 11, 4–9.

Rachocki, A. (1981). *Alluvial fans*, Wiley, New York.

Sambrook-Smith, G. H., and Ferguson, R. I. (1995). "The gravel-sand transition along river channels." *J. Sed. Res.*, A65(2), 423–430.

Schumm, S. A., Mosley, M. P., and Weaver, W. E. (1987). *Experimental fluvial geomorphology*, Wiley, New York.

Zarn, B., and Davies, T. R. H. (1994). "The significance of processes on alluvial fans to hazard assessment." *Zeit. Geomorph. N. F.*, 38, 488–500.